Combustion and Flame 159 (2012) 1732–1740

Contents lists available at SciVerse ScienceDirect

Combustion and Flame

journal homepage: www.elsevier.com/locate/combustflame

Combustion of nanofluid fuels with the addition of boron and iron particles at dilute and dense concentrations

Yanan Gan, Yi Syuen Lim, Li Qiao *

School of Aeronautics and Astronautics, Purdue University, West Lafayette, IN 47907, United States

ARTICLE INFO

Article history:
Received 17 August 2011
Received in revised form 3 November 2011
Accepted 9 December 2011
Available online 7 January 2012

Keywords:
Nanofluid fuels
Droplet combustion
Energetic nanoparticles
Boron
Iron
Water absorption

ABSTRACT

The combustion characteristics of nanofluid fuels containing additions of boron and iron particles were investigated. The effects of particle materials, loading rate, and type of base fuel on suspension quality and combustion behavior were determined. The burning behaviors of dilute and dense suspensions were compared, and the results for dense nanosuspensions showed that most particles were burned as a large agglomerate at a later stage when all the liquid fuel had been consumed. Sometimes this agglomerate may not burn if the energy provided by the droplet flame is insufficient. For dilute suspensions, the burning characteristics were characterized by a simultaneous burning of both the droplet and the particles, which integrated into one stage. The fundamental mechanism responsible for bringing the particles out of the droplet, which is a prerequisite condition for them to burn, is different for n-decane- and ethanol-based fuels. For the former, the particles are brought out of the droplet by a disruptive behavior of the primary droplet, which was characterized by multiple-time disruptions and with strong intensity. This was caused by the different boiling points between n-decane and the surfactant. For ethanol-based fuels having no added surfactant, the particles are also brought out of the droplet by disruptive behavior, but characterized by continuous disruptions of mild intensity. This was very likely caused by a continuous water absorption by the ethanol droplet during its burning process.

© 2011 The Combustion Institute. Published by Elsevier Inc. All rights reserved.

1. Introduction

Nanofluid fuels, a new class of nanotechnology-based fuels, are liquid fuels with a stable suspension of nanometer-sized particles. Depending on the physical, chemical, and electrical properties of the added nanomaterials, nanofluid fuels can achieve better performance, e.g., increased energy density, easier and faster ignition, enhanced catalytic effects, and improved combustion efficiency. Certain drawbacks such as strong particle aggregation and potential emissions of metal and metal oxide particles may limit applications of nanofluid fuels [1]. Nevertheless, nanofluid fuels have been rarely studied, and our knowledge about them remains very limited.

Tyagi et al. [2], using a simple hot plate experiment, reported that the ignition probability of diesel fuel containing a small amount of aluminum nanoparticles was significantly higher than that of pure diesel fuel. Using a shock tube, Jackson et al. [3] found that an addition of aluminum nanoparticles could substantially decrease the ignition delay time of n-dodecane above 1175 K. This was further evidenced by Allen et al. [4], who used an aerosol shock tube to find that an addition of 2% (by weight) aluminum nanoparticles in ethanol can reduce the ignition delay by 32.0%, also that this reduction is even higher for JP-8. Sabourin et al. [5] recently studied the combustion of monopropellant nitromethane containing colloidal particles of functionalized grapheme sheets and found that the burning rate was significantly increased even with an additive of 1.0 wt%. Young et al. [6,7] evaluated the potential of nano-sized boron particles as fuel additives for high-speed airbreathing propulsion. Their results show that boron particle can be successfully ignited in an ethylene/oxygen pilot flame. However, a critical temperature around 1770 K must be reached above which sustained combustion of boron particles can be achieved. Van Devener and Anderson [8] conducted the first study of the catalytic combustion of JP-10, using soluble CeO_2 nanoparticles as the catalyst. Their results show that the ignition temperature of JP-10 was significantly reduced. The group later developed a unique process which produced air-stable unoxidized boron nanoparticles that are coated with a combustion catalyst ceria [9,10]. These nanoparticles are soluble in hydrocarbons and could be used as fuel additives because of the dual effects – high energy density of the core component boron and catalytic effect of the outside layer. Rotavera et al. [11] found that the presence of CeO_2 nanoparticles in toluene significantly reduces soot deposition on the shock-tube wall under the conditions of high fuel concentration.

* Corresponding author. Address: 701W. Stadium Ave., West Lafayette, IN 47907-2045, United States. Fax: +1 1 765 494 0307.
E-mail address: lqiao@purdue.edu (L. Qiao).

0010-2180/$ - see front matter © 2011 The Combustion Institute. Published by Elsevier Inc. All rights reserved.
doi:10.1016/j.combustflame.2011.12.008

The combustion of nanofluid fuels is a highly complex phenomenon, which is a multiphase, multicomponent, and multiscale process. The fuel itself contains liquid and solid particles, and its colloidal stability depends largely on the interfacial properties between the particle and the surrounding fluid molecules. Multiple physical and chemical processes will take place during the combustion of nanofluid fuels, and these processes can interact with one another to make our fundamental understating even more difficult. They include evaporation of the liquid fuel, combustion of the liquid fuel in vapor phase, combustion of the solid particles, mass and energy transfer between the phases, dynamics of the particles, and other combinations. Moreover, the physical properties of nanofluid fuels can be very different from the base fuels. For example, nanofluids have significantly increased thermal conductivity as a result of the random Brownian motion of nanoparticles in liquid [12–14]. Furthermore, the radiation properties (by absorption) of nanoparticles could also aid combustion.

Motivated by this, Gan and Qiao [1] recently investigated the burning characteristics of fuel droplets containing suspended nano- and micron-sized aluminum particles. The results show that for the same solid loading rate and surfactant concentration, the microexplosive behavior of micron suspensions occurred more intensely compared to nanosuspensions, thus providing a means of efficient and more complete burning of particles. The characteristics of the particle aggregate formed during combustion were found to be responsible for the different burning behaviors: the nanosuspension resulted in a dense, porous aggregate, and the micron suspension resulted in a rigid, impermeable aggregate. Moreover, the authors showed that for nanosuspensions the dominant mechanism for aggregation is the Brownian motion, but for micron suspensions it is fluid transport, such as droplet surface regression and internal circulation.

Although our previous paper [1] focused on the effects of particle size (nano vs. micron) in regard to the overall droplet combustion characteristics, the present one focuses on the effects of particle material and concentration. Metals other than aluminum, such as boron, iron, magnesium, and titanium, are also commonly used in solid propellants and explosives because of their high combustion energy. For example, the maximum combustion enthalpy of boron is almost two times higher than that of aluminum [15]. If boron can be properly mixed and burned with liquid fuels, higher volumetric energy density can be expected. However, boron has different physical and chemical properties than aluminum does, such as a higher melting point. Therefore the burning characteristics are different. Moreover, our previous work about nanofluid fuels deals with relatively dense particle loading rates, typically above 10.0 wt%. At such concentrations, the overall burning behavior is largely affected by the particle aggregation process. At dilute concentrations, however, the aggregation behavior may not be that serious – particles will take a much longer time to form an aggregate (by collisions) in comparison to dense suspensions. This would provide an opportunity to study the interactions between the liquid and the individual particles by limiting particle aggregation to a minimum. This would especially help us to understand the mechanisms of how particles can escape from the liquid, which is necessary for them to burn, for the sake of increasing the energy density of the liquid fuel.

Motivated by above, the burning characteristics of nanofluid fuels with the addition of boron and iron particles was investigated in this paper. The effect of particle-loading rate on droplet-burning characteristics was examined. The fundamental mechanisms responsible for particles escaping from the primary droplet were discussed.

2. Experimental methods

2.1. Fuel preparation and characterization

The methodology to physically and chemically disperse particles evenly in liquid fuels and to minimize particle agglomeration was discussed in a previous study [1]. Here we will only briefly describe the preparation process. The particles were first vigorously mixed with the base fuel by hand, and an ultrasonic disruptor was then used to prevent particle agglomeration. This was performed in an ice bath. We usually add a surfactant, Sorbitan Oleate, to the mixture to promote chemical stabilization of the suspension.

Two liquid fuels, n-decane and ethanol, were considered as the base fluid. As a typical saturated alkane fuel and a typical alcohol fuel, n-decane and ethanol, have quite different physical properties [1]. Boron and iron particles were considered as additives to the base fuel. Their physical properties are listed in Table 1 [16]. The amount of particles to be added to the liquid fuel was determined by using an analytical scale (Torbal AGZN 100) with an accuracy of 0.1 mg.

Figure 1a shows a Scanning Electron Microscope (SEM) image of iron nanoparticles with an average size of 25 nm, purchased from Nanostructured & Amorphous Materials, Inc. These particles were coated with a thin layer of carbon about 2–6 nm thick to prevent oxidation. Most iron particles are spherical and uniform, and the size distribution ranges from 15 to 80 nm. Boron nanoparticles (80 nm) were purchased from Skyspring Nanomaterials, Inc., in amorphous form. As seen in Fig. 1b, these particles have a non-spherical shape and tend to agglomerate.

We then examined the suspension quality of various nanofluid fuels. The surfactant concentration was kept at 0.5 wt% for nanofluids with n-decane as base fluid. No surfactant was added for nanofluids with ethanol as base fluid. The suspension quality was evaluated by counting the settling time – how long it took for particles to completely settle on the bottom of the test tube after preparation of the nanofluid. Overall, for the same amount of surfactant, the suspension quality of nanoparticles at dilute concentrations is better than that at dense concentrations. Boron nanoparticles (80 nm) have a better suspension quality than iron nanoparticles in n-decane. This is because iron has a much higher density (7.87 g/cm^3) than boron (2.34 g/cm^3). With ethanol as the base fuel, nanoparticles have a much better suspension quality than in n-decane. For example, boron nanoparticles (0.5 wt%) can maintain good suspension for more than 4 h in ethanol without adding a surfactant, while they settle in about 15 min in n-decane when a surfactant is used. This is because ethanol is a polar and hydrophilic liquid. Thus, good suspension of nanoparticles with hydrophilic oxide surface in ethanol can be maintained. For non-polar and hydrophobic solvent such as n-decane, however, particle

Table 1
Bulk physical properties of aluminum, boron, and iron particles.

	Density (g/cm^3)	Melting point (K)	Boiling point (K)	Passivated layer or oxide	Melting point (K)	Boiling point (K)
Boron	2.34	2349	4200	B_2O_3	723	2133
Iron	7.87	1811	3134	Fe_2O_3	1839	–
Aluminum	2.70	933	2792	Al_2O_3	2345	3250

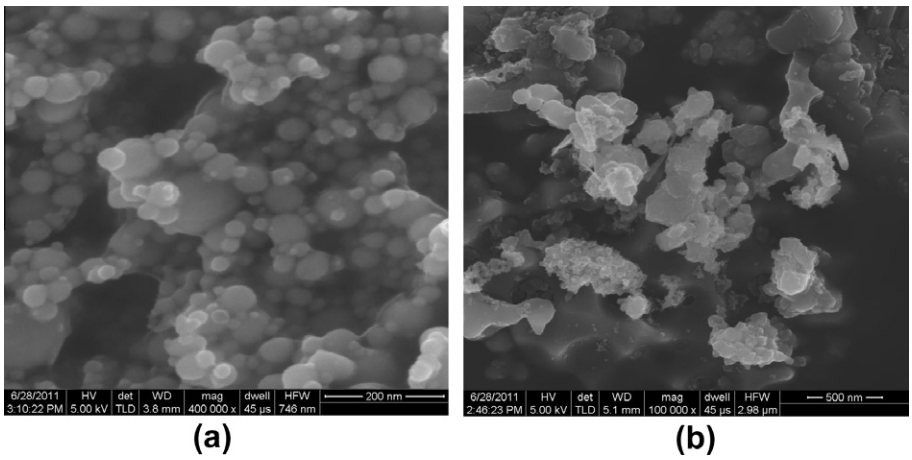

Fig. 1. SEM photographs of (a) nano-sized iron particles with a mean size of 25 nm and (b) nano-sized boron particles with a mean size of 80 nm.

surface modification with a surfactant is needed to achieve good suspension [17].

2.2. Experimental setup

The experimental setup was described in detail in our previous paper [1]. Briefly, the experiments were performed in a closed chamber with quartz windows for optical access. The droplet was suspended on a silicon carbide (Si–C) fiber (78 μm in diameter), which has low thermal conductivity (5.20 W/m K at 300 K). The heat loss from the fiber can be neglected during much of the droplet life time if the fiber size is less than 100 μm [18]. A heating wire that was attached to a solenoid device was used to ignite the droplet, and moved away right after the droplet was ignited. The droplet burning process was recorded by a high-speed digital camera with a framing rate of up to 10,000 fps. Weak backlight was also used for better visualization of the droplet and its breakup process.

3. Results and discussion

We have previously investigated the combustion characteristics of fuel droplets containing suspended nano- and micron aluminum particles at relatively dense loading rates [1]. In the following sections, we will discuss the effect of boron and iron particles on the combustion characteristics of nanofluid fuel droplets. For ignition and combustion of energetic particles, the oxide layer around the particles has to be melted first. After removal of the oxide layer, the active content inside will be melted and reacted [19]. Thus, the melting point and boiling point of the metal oxide and the meal will fundamentally influence the combustion behavior of individual particles. Because the chemical and physical properties of boron and iron are different from those of aluminum, as compared in Table 1, the overall burning characteristics of these particles in nanofluids are expected to be different.

3.1. Combustion of droplets with the addition of boron particles

In the following we will discuss the overall burning characteristics of n-decane- and ethanol-based fuel droplets containing boron particles at dense loading rates (5–20 wt%).

3.1.1. Boron particles in n-decane-based fuels

Figure 2 shows the burning sequence of an n-decane droplet with the addition of boron nanoparticles (80 nm) at a particle loading rate of 5.0 wt%. The surfactant concentration is 0.5 wt%. After ignition (Fig. 2a), a steady envelope flame was established around the droplet. A few particles were ignited and burned during this stage (Fig. 2b). When the droplet size decreased to a critical value, more particles were ignited and many individual particle flames were observed, as shown in Fig. 2c. These flames were recognized by the bright spots around the droplet and the envelope flame. As the droplet became smaller, the burning of individual particles intensified. Until the end, nearly all particles were burned

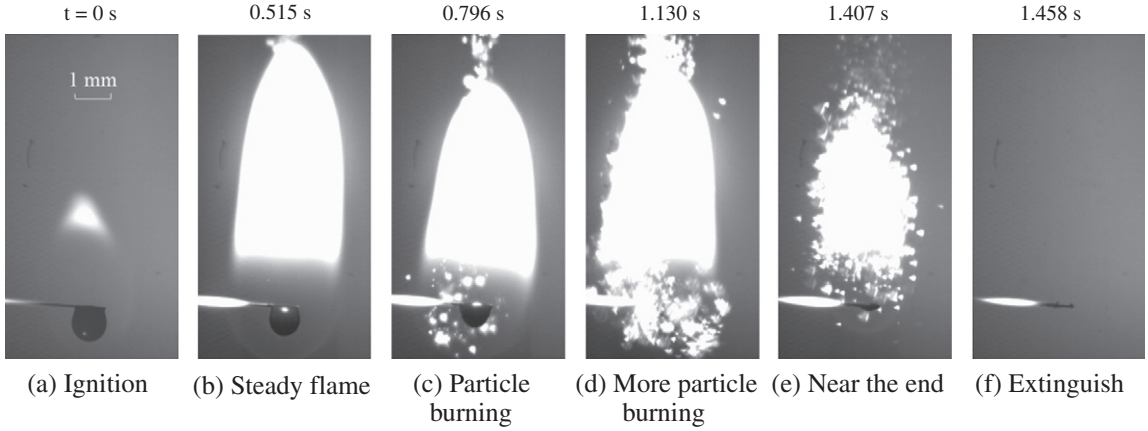

Fig. 2. A burning sequence of an n-decane/nano-B droplet. The particle (80 nm) concentration is 5.0 wt%. The surfactant concentration is 0.5 wt%.

altogether with the droplet; as shown in Fig. 2f, and no obvious agglomerate was left on the fiber.

During the burning process, we observed multiple disruptions of the primary droplet. This is because the droplet is a mixture of n-decane and surfactant, which have very different boiling points. During each disruption, the droplet oscillated, the droplet flame was distorted, and smaller droplets were ejected from the primary droplet. This provided a means to transport boron particles out of the primary droplet. The particles were then ignited and burned when they got close to the flame zone; the temperature there was high enough to melt the oxide layer, and the oxygen was able to diffuse onto the particle surface.

With 5.0 wt% boron in an n-decane droplet, no obvious agglomerate was left on the fiber, indicating that the burning of the boron particles took place simultaneously with the burning of the droplet. We then conducted experiments at higher particle concentrations, up to 20.0 wt%. The results show that the burning process is similar to the 5.0 wt% example, except that at a later stage an agglomerate was observed forming on the fiber after the liquid fuel was consumed. The boron agglomerate, however, sometimes did not ignite after the envelope flame was extinguished. In summary, at high particle loading rates a small portion of the boron particles were burned as individual particles during the early stages as a result of being ejected from the primary droplet multiple times. The rest would form a large agglomerate, which may or may not ignite when the droplet flame was gone, depending on the intensity and frequency of the microexplosions that had happened previously.

3.1.2. Boron particles in ethanol-based fuels

As discussed earlier [1], surfactant plays an important role in the combustion behavior of the multiple-component droplets. The different boiling points between the surfactant and the base fuel can result in disruption and a microexplosion of the primary droplet, with many smaller droplets being ejected from the primary one. Obviously, adding a surfactant would complicate the overall burning process. The effect of the surfactant on droplet combustion of boron slurries has been studied previously [20–23], and these studies considered high concentrations of micron-sized boron particles. These studies show that the pyrolyzed surfactant bounds the boron particles and forms an impermeable shell structure. Due to pressure build-up inside the structure, the shell will finally explode and micro-explosion behavior happens.

For the experiments of boron particles in ethanol-based fuels, which we will discuss below, we added no surfactant. This is because boron particles can be well-suspended in ethanol for a long time without the use of a surfactant. Figure 3 shows the burning sequence of an ethanol droplet with 5.0 wt% boron particles (80 nm). The exposure time of the camera was set to be 200 μs to better show the ignition and combustion process of particles. Note that the ethanol envelope flame was quite weak and can hardly be observed. There are several differences between the combustion characteristics of ethanol and n-decane based fuel droplet.

Firstly, upon droplet ignition, the boron particles were immediately transported to the flame zone, as shown in Fig. 3a. For n-decane-based droplet (Fig. 2), however, a delay occurred between the droplet ignition and the ignition of particles. Secondly, boron particles escaped continuously from the primary ethanol droplet but periodically from n-decane-based droplet, accompanying disruptions of the primary n-decane droplet. Lastly, compared with the disruptions from n-decane based droplet, we observed disruptions from ethanol-based droplet occur continuously but with much lower intensity.

Figure 4 shows SEM images of the combustion residue of the ethanol-based fuel. (This agglomerate was left on the fiber after combustion was completed.) The overall view shows that the agglomerate was smooth and spherical, but slightly distorted because of interference with the supporting fiber. A magnified view of the agglomerate surface reveals that the surface texture differs at various locations. For example, the surface in area A is smooth; no individual particles can be identified – they agglomerated together. The surface in area B, however, is rough, composed of individual particles. Energy Dispersive X-ray Spectroscopy (EDX) analysis was conducted at multiple points in areas A and B to better understand the local composition. The atom numbers of boron and oxygen at each area were averaged from the data at multiple locations. The results show that the boron-to-oxygen atom ratio in area A is much lower than in area B (1.278 vs. 4.450). This indicates that the particles in area A may have been partially oxidized. Note, however, that we observed no ignition and burning of the large boron agglomerate at a later stage (we did observe this, however, for an ethanol droplet containing suspended aluminum nanoparticles), which may be because the heat provided by the droplet flame was insufficient.

3.1.3. Mechanisms of boron ignition and combustion

The discussions so far have focused on the overall burning characteristics of fuel droplets containing suspended boron particles. We will now discuss the ignition and combustion mechanisms of boron particles during droplet combustion. Here we used a Nikon

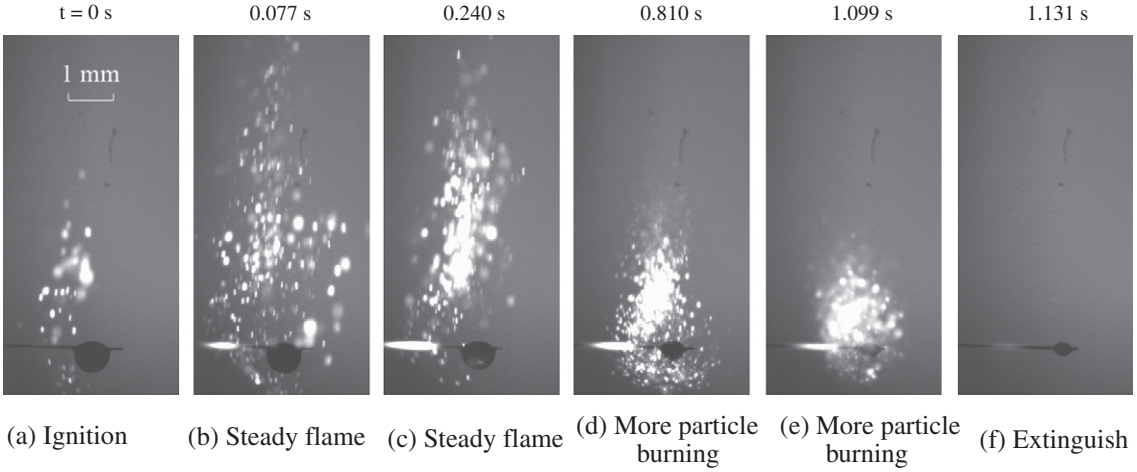

Fig. 3. A burning sequence of an ethanol/nano-B droplet. The particle (80 nm) concentration is 5.0 wt%.

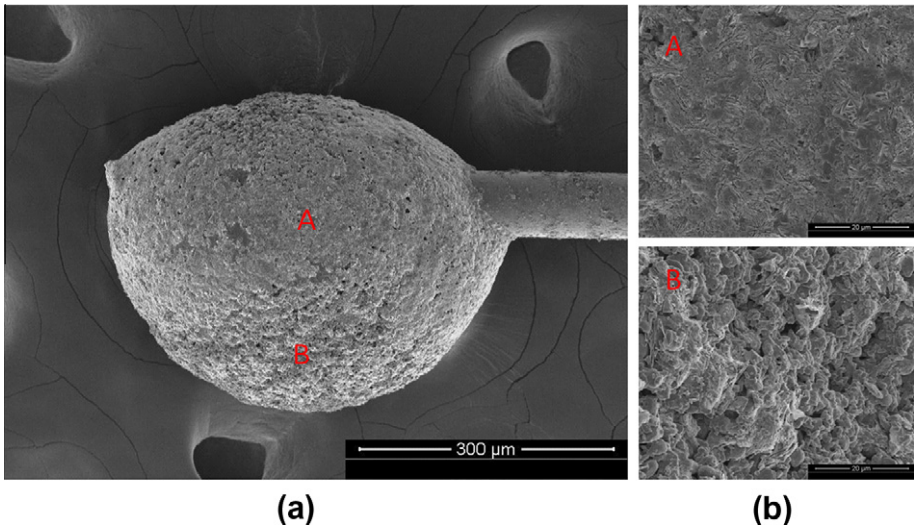

Fig. 4. SEM photographs of the combustion residue (an agglomerate) of an ethanol/nano-B droplet. The particle (80 nm) concentration is 5.0 wt%.

DSLR camera (D40 with a resolution of 3008 × 2000) coupled with a micro lens to capture the ignition and burning process of boron particles. The framing rate of the camera was set at 3 frames per second, and the exposure time was set at 8 ms. The long exposure time helped to illustrate the emissions from the flame.

Figure 5 shows a sequence of pictures taken by the DSLR camera for an ethanol droplet with boron micron particles (5.0 wt%). The flame structure was characterized by a blue envelope flame around the droplet. The blue flame sheet indicates the flame front where ethanol vapor reacts with oxygen in the air. Multiple streaks were observed on the top of the envelope flame, which indicates the ignition and burning of boron particles. A magnified view of a single particle flame was shown in Fig. 5d. The yellow zone at the bottom of the flame indicated ignition of the particle. Combustion of it was characterized by the bright white zone in the middle with green emission around it. The top orange and red part indicated the cooling-down process after the particle was burned. These observations are consistent with those by Li and Williams [24] on the combustion of single boron particles. The green emission around the combustion zone in Fig. 5d is the emission from the combustion product BO_2. For the droplet flame (Fig. 5b and c), the green emission is mostly located at the top of the envelope flame.

According to the classical model [25], the combustion of a boron particle typically involves two stages. The first one is associated with the burning of boron while the oxide layer is still around the particle. The heat will melt the outer layer of oxide (B_2O_3), and oxygen will diffuse in and react with the active boron inside. The heat release from the heterogeneous reaction may provide enough energy to vaporize the melted oxide layer. The second stage will be initiated after the oxide layer is gone by vaporization from the active boron surface. This stage is characterized by the bare boron reaction with oxygen. This is consistent with what we have observed in Fig. 5d: the yellow zone at the bottom of the particle flame indicates the first stage of boron particle combustion when the oxide layer is still being melted, and oxygen reacts with the boron through diffusion. At this stage, the temperature of the particle is not high enough, and less BO_2 is emitted. This results in a yellow flame without green emission around it. The second stage of boron particle combustion is demonstrated by the bright white zone. In this stage, bare boron reacts with oxygen as the oxide layer is vaporized away. The particle temperature is high, and more BO_2 is produced. This explains the bright white flame and the strong green emission around it.

Figure 6 shows a sequence of pictures taken by the DSLR camera for an n-decane-based droplet with boron particles (5.0 wt%). The

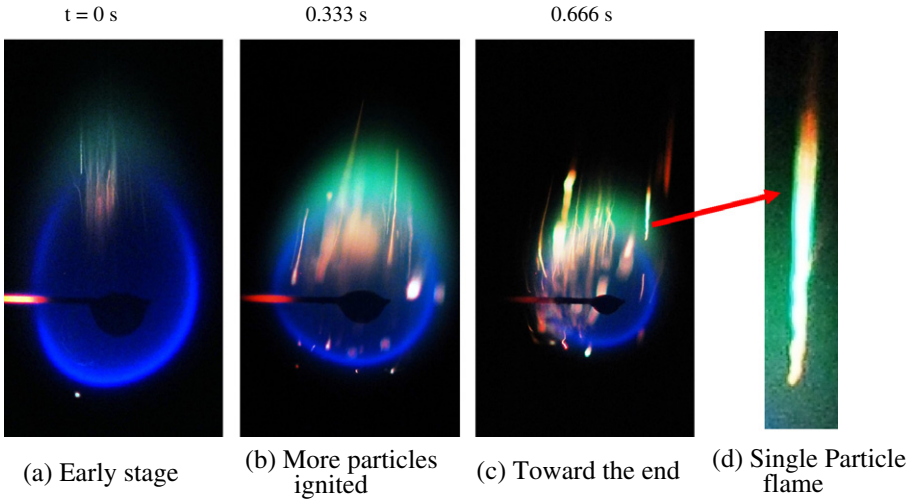

Fig. 5. Successive pictures of boron particle (5.0 wt%) ignition and burning in an ethanol-based fuel droplet.

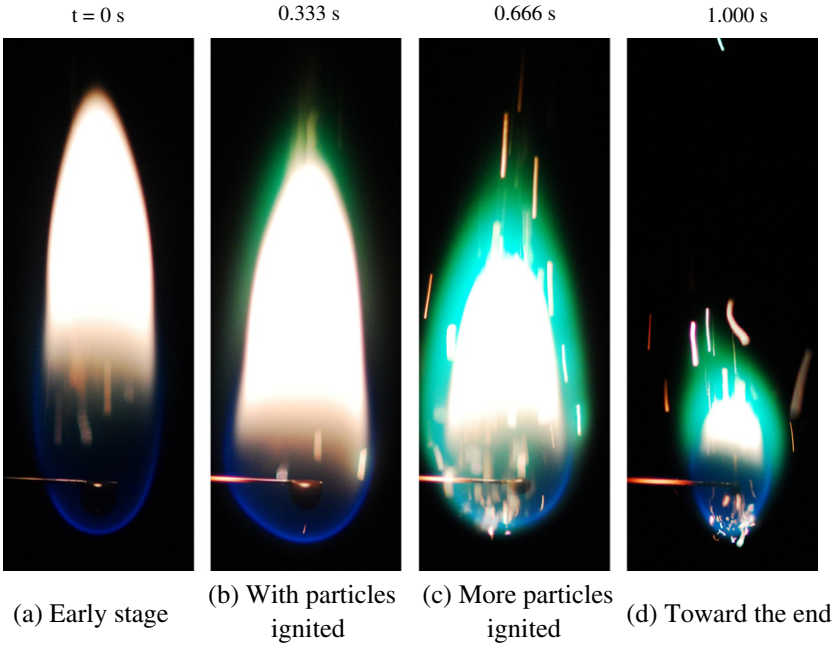

Fig. 6. Successive pictures of boron particle (5.0 wt%) ignition and burning in an n-decane-based fuel droplet.

flame structure was characterized by a blue flame sheet at the bottom and a sooty flame zone at the top. Similarly, boron particle ignition and combustion were indicated by the streaks. A green zone, which indicates emission of BO_2, surrounds the entire envelope flame, as shown in Fig. 6c. This zone is wider than that of an ethanol droplet, which appears only atop the envelope flame. This might be because of the higher temperature of the n-decane droplet flame.

3.2. Combustion characteristics of droplets with the addition of iron particles

3.2.1. Iron particles in n-decane-based fuels

The burning sequence of an n-decane-based droplet with 5.0 wt% iron nanoparticles is shown in Fig. 7. Similar to the droplet with boron nanoparticles, a steady envelope flame was formed around the droplet shortly after ignition; this flame is shown in Fig. 7a and b. During this process, few iron particles escaped from the droplet. When the droplet size decreased to a critical value, iron particles, along with smaller droplets, were ejected from the primary droplet and ignited and burned, as shown in Fig. 7c. The locations where ignition occurred are near the flame zone. The trajectory of the particles basically followed the direction of the ejection of the smaller droplets, as shown in Fig. 7c. Similar to an n-decane droplet containing boron particles, iron particle ignition and subsequent combustion were a result of disruption of the primary droplet, by which smaller droplets, which contain particles, were ejected to the hot flame zone. More particles were ignited as the droplet size became smaller. As shown in Fig. 7d, the ignition and burning of individual particles or particle aggregates were characterized by small bright sparks. Later, a "dried" agglomerate started to form on the fiber, shown in Fig. 7e. Once the envelope flame was extinguished, the agglomerate melted and then burned on the tip of the fiber.

The combustion residue was characterized by a brown agglomerate loosely attached to the tip of the fiber. An SEM photograph of the residue was shown in Fig. 8. The overall structure was characterized by the exploded holes, which had resulted from the multiple microexplosions of the primary droplet because of the different boiling points between n-decane and surfactant.

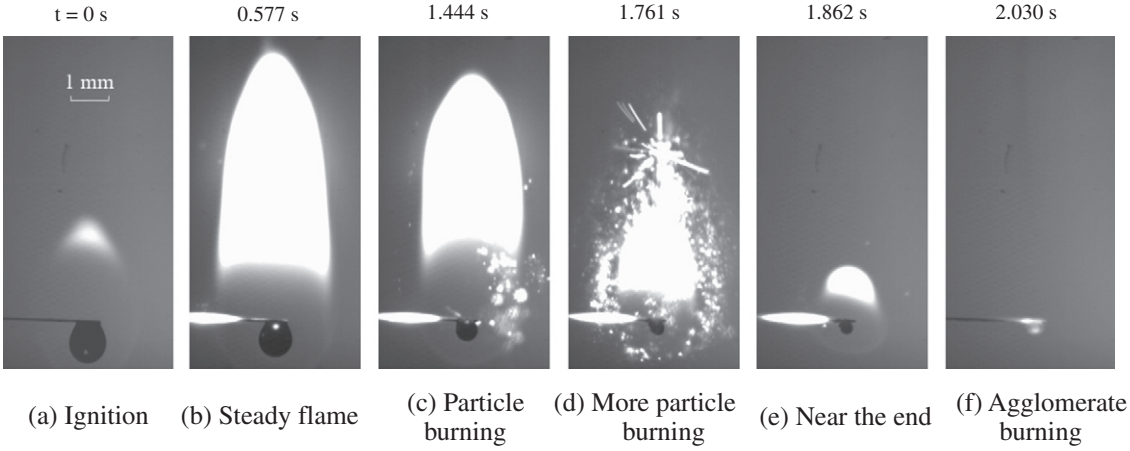

Fig. 7. A burning sequence of an n-decane/nano-Fe droplet. The particle (25 nm) concentration is 5.0 wt%. The surfactant concentration is 0.5 wt%.

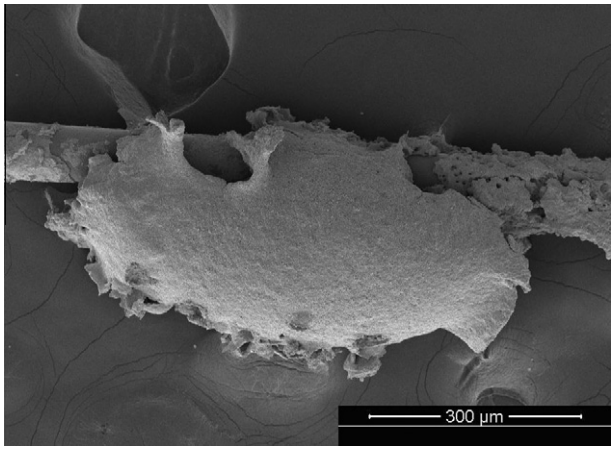

Fig. 8. SEM photographs of the combustion residue (an agglomerate) of an n-decane/nano-Fe droplet. The particle (25 nm) concentration is 5.0 wt%.

3.2.2. Iron particles in ethanol-based fuels

Figure 9 shows the burning sequence of an ethanol droplet with 5.0 wt% iron particles (25 nm). Note that for these experiments, we added no surfactant to the mixture. Again, the droplet burning characteristics of the ethanol-based fuels is quite different from that of the n-decane-based fuels (Fig. 7). The chief difference is that particles were continuously ejected from the primary droplet and transported to the flame zone where they were ignited and burned. For the n-decane-based fuels, however, the ignition and subsequent burning of particles was accompanied by each disruption of the primary droplet. This difference, as a result of different base fuels (n-decane vs. ethanol), is consistent with our previous observations for droplets with the addition of boron particles. We will explain this in Section 3.4.

3.2.3. Mechanisms of iron particle ignition and combustion

We observed that iron particle ignition and combustion processes are somehow different from those of boron and aluminum. Figure 10 shows an image of a burning ethanol droplet and a burning of individual iron particles. The ethanol flame was weak and cannot be readily seen unless under high exposure time. Here we kept the exposure time at 200 μs to see the ignition and combustion process of iron particles. We can see in Fig. 10a that iron particle burning was characterized by individual particle flames shown by the bright spots, and some of these spots were rather large. The distribution of the particle flames surrounds the ethanol envelope flame, which means that iron nanoparticles can be ignited and burned only near or within the flame zone.

Some particles (most likely large particle aggregates) exploded shortly after ignition, forming jets in multiple directions, as shown in Fig. 10b. This process happened quickly and aggressively and has similarities to particle jetting in metalized explosives [26]. This phenomenon, which was not observed with aluminum or boron, is very likely because iron particles are heavy and agglomerate quickly in liquid. Thus the smaller droplets and particles ejected from the primary droplet may contain large aggregate structures. A small amount of liquid fuel may be trapped inside the iron particle aggregates. When such aggregates are ejected to the flame zone, quick vaporization of the liquid fuel and potential pressure build-up inside the agglomerate may cause intense breakup of the aggregate and form jetting in multiple directions.

3.3. Effect of particle concentration

The results show that for nanosuspensions at high particle loading rates, a large agglomerate will form on the supporting fiber at the later stage. Most of the particles will be ignited as this agglomerate and burned at a later stage once all the liquid fuel has been consumed, e.g., nano-Fe in n-decane. Sometimes, however, the large agglomerate may not be ignited and burn if the energy provided by the droplet flame is insufficient to melt the oxide layer, e.g., nano-B in ethanol. For suspensions with micron- or larger-sized particles at high particle-loading rates, most particles are burned during the microexplosion event in which the particle aggregate exploded suddenly. The microexplosion phenomenon provides an efficient means of burning particles.

In the following, the burning characteristics of dilute suspensions (particle mass concentration <1%) will be discussed. To avoid the complicated burning process resulting from the addition of a surfactant and to focus on the effects of particle concentration, we chose ethanol as a base fuel because the suspension quality is very good even without a surfactant. The burning characteristics of dilute suspensions are very different from those of dense suspensions. For the latter, when a surfactant was not added, the burning process can be divided to two separate stages: a droplet combustion stage followed by a particle-agglomerate burning state. For dilute suspensions, the burning process is characterized by simultaneous burning of both the liquid and particles, integrated into one stage. We observed that the particles continuously escaped from the surface of the droplet, reaching the flame zone where the temperature is high and there is more oxygen. The particles were then ignited and burned, rising as a result of natural

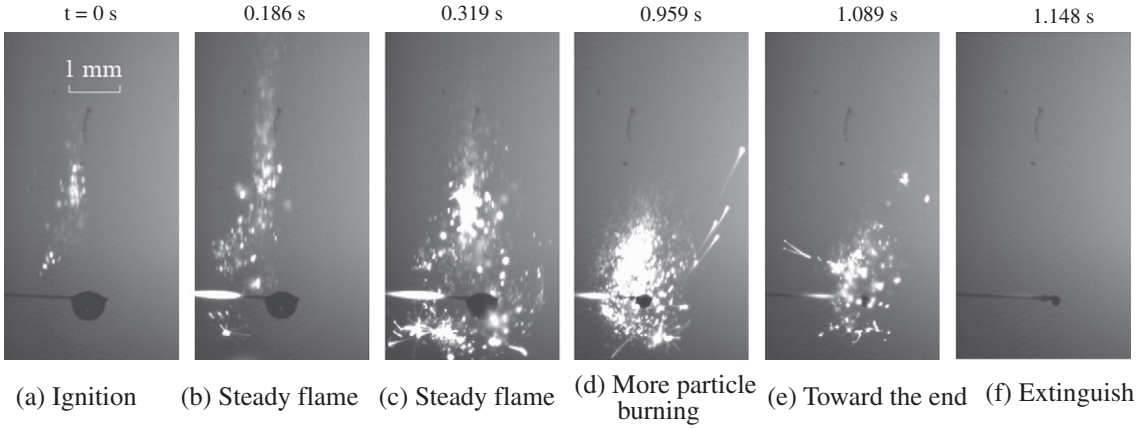

Fig. 9. A burning sequence of an ethanol/nano-Fe droplet. The particle (25 nm) concentration is 5.0 wt%.

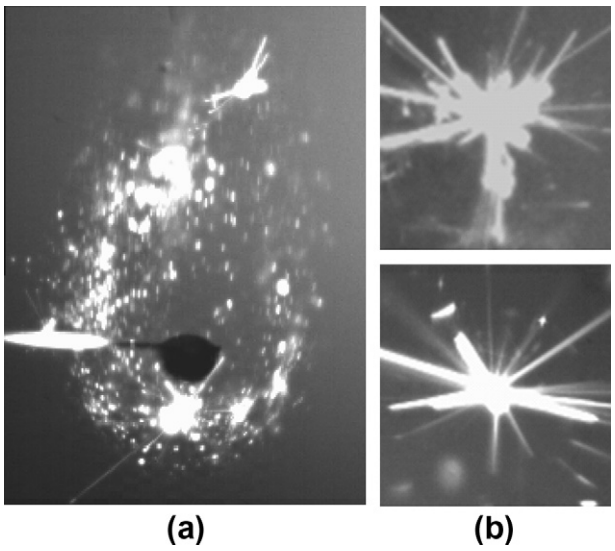

Fig. 10. (a) An image of the combustion of an ethanol-based fuel droplet with 5.0 wt% iron nanoparticle. (b) A magnified view of iron particle explosion.

convection. No particle agglomerate or combustion residue was left on the fiber.

The different burning behaviors at dense and dilute loadings can be explained by particle transport and dynamics inside the droplet. Under dense loading rates, it is easier and quicker to form an aggregate. Because of the strong tendency of agglomeration, individual particles have little chance to move to the droplet surface and then escape from the surface. Under a dilute loading rate, however, without the strong tendency of agglomeration, particles can have a chance to escape from the droplet to burn. However, the big question that remains is this: How can particles escape from a droplet that must counteract the surface tension force? This will be discussed in the next section.

3.4. Mechanisms of particle escaping from the droplet

We have explained earlier that when a surfactant is added to the base fuel, such as n-decane, a disruption of the primary droplet occurs as a result of the different boiling points of the two fluids, and smaller droplets are ejected from the primary one. This provides a means of bringing particles out of the droplet and transporting them to the hot flame zone where they can be ignited. We did observe that the ignition and burning of particles were accompanied by each disruption event. The disruption happened multiple times with strong intensity, which is because of the large difference between the boiling points of n-decane and the surfactant. Therefore the multicomponent nature of the droplet, which results in disruptions, seems to be the only mechanism that could bring the particles out of the droplet.

However, for pure ethanol-based droplets, for which no surfactant was added, we also observed the "integrated" burning behavior that particles and the droplet were burned simultaneously, and the particles were able to continuously escape to the hot flame zone. Moreover, the primary droplet experienced continuous disruption, but the intensity is much lower in comparison to that of the n-decane/surfactant droplet. Therefore the integrated burning behavior of ethanol droplets seems also to be a result of continuous disruptions. But why do disruptions occur for pure ethanol droplets?

We believe they were caused by water vapor absorption by the ethanol droplet. According to an early study by Lee and Law [27], the water vapor from the droplet flame and the surrounding atmosphere can freely condense on the ethanol droplet surface and then dissolve into the droplet. The mass percentage of the absorbed water in an ethanol droplet can go up to more than 50% toward the end of the combustion process. The absorption of water, a continuous process, causes the droplet to become a multicomponent. Based on the classical theory of multicomponent droplet combustion [28], the more-volatile component (ethanol in this process) will be vaporized first. Ethanol is more volatile compared to water, since ethanol (352 K) has a slightly lower boiling point (373 K). Thus the droplet surface is more concentrated with a less-volatile component, which here is water. The superheat accumulated will result in nucleation of ethanol inside the droplet, and the bubbling of ethanol will create a pressure buildup, finally resulting in a breakup of the primary droplet. However, this droplet breakup was not a global and catastrophic explosion because the boiling points of ethanol and water are not very different (352 K vs. 373 K). The breakup occurs mildly, but with a higher frequency, thus resulting in a continuous ejection of smaller droplets from the primary droplet. Particles can therefore be continuously transported to the flame zone all around the droplet, resulting in the integrated burning behavior.

Furthermore, the existence of the supporting fiber could be partially responsible for the droplet-burning behaviors. Heterogeneous nucleation because of the fiber can result in small-droplet ejections, and particles in them will ignite when they get close to the flame zone. In this sense, combustion of free-fall droplets would be better. Also, it is possible that alcohol fuels can dehydrate with the existence of a catalyst. For example, the aluminum samples we used in the experiments are coated with an Al_2O_3 layer, which could catalyze dehydration of alcohols. According to a study by Knozinge [29], such dehydration reactions take place at temperatures ranging from 513 K to 523 K. These temperatures are close to the droplet temperature measured by a thermocouple in our experiment [1], indicating that the dehydrating reactions can take place with the presence of Al_2O_3. The potential production of water and diethyl ether ($(C_2H_5)_2O$) as a result of the dehydration reactions would enhance the disruption behavior of the primary droplet, causing particles to be ejected from it. Nevertheless, more investigation is needed on the potential catalytic effect of these nanoparticles.

4. Conclusion

The combustion characteristics of nanofluid fuels containing boron and iron particles were investigated at high and low concentrations. The leading conclusions are:

(1) For dense suspensions containing boron nanoparticles, some particles were ignited and burned simultaneously with the burning of the liquid fuel. The rest of them formed a large agglomerate on the fiber at a later stage as a result of particle aggregation. This agglomerate may or may not burn, depending on the base fluid. For example, the agglomerate sometimes was able to ignite for n-decane-based fuels, but not for the ethanol-based fuels because the droplet temperature is higher for the former, which could provide sufficient energy to melt the agglomerate. Moreover, the ignition and burning process of individual boron particles were observed. The emission of the combustion product was characterized by green emission from BO_2.

(2) For dense suspensions containing iron nanoparticles, similar behavior was observed: part of the particles was burned simultaneously with the liquid droplet, and the rest formed a large agglomerate on the fiber at a later stage. The agglomerates were able to ignite and burn for the n-decane and ethanol-based droplets. Some iron particles (most likely large particle aggregates) exploded shortly after ignition, forming

jets in multiple directions. This behavior, which was not observed with aluminum or boron, is very likely due to the iron particles being heavy and agglomerating quickly in liquid. When these large aggregates were emitted and ignited, heat could cause instabilities on particle surfaces, resulting in aggregate breakups and the formations of jets in multiple directions.

(3) For dilute suspensions, when a surfactant was not added the burning characteristics of ethanol-based fuels were characterized by simultaneous burning of both the droplet and the particles, which integrated into one stage. The particles were able to continuously escape from the droplet surface and were then transported to the flame zone where they were ignited.

(4) The fundamental mechanisms responsible for bringing particles out of the droplet, which is a prerequisite condition for them to burn, is different for n-decane and ethanol-based fuels. For the former, the particles are brought out by the disruptive behavior of the primary droplet, which was characterized by multiple disruptions with strong intensity caused by the different boiling points between n-decane and surfactant. For ethanol-based fuels without a surfactant being added, however, the particles are also brought out of the droplet by disruptive behavior, which was characterized by continuous disruption at mild intensity, very likely caused by the continuous water absorption by the ethanol droplet during its burning process.

Acknowledgments

This work has been supported by the Army Research Office (ARO) with Dr. Ralph Anthenien as the technical monitor.

References

[1] Y. Gan, L. Qiao, Combustion and Flame 158 (2011) 354–368.
[2] H. Tyagi, P.E. Phelan, R. Prasher, R. Peck, T. Lee, J.R. Pacheco, P. Arentzen, Nano Letters 8 (2008) 1410–1416.
[3] D. Jackson, R. Hanson, in: 44th AIAA/ASME/SAE/ASEE Joint Propulsion Conference and Exhibit, Hartford, CT, 2008.
[4] C. Allen, G. Mittal, C.J. Sung, E. Toulson, T. Lee, Proceedings of the Combustion Institute 33 (2011) 3367–3374.
[5] J.L. Sabourin, R.A. Yetter, B.W. Asay, J.M. Lloyd, V.E. Sanders, G.A. Risha, S.F. Son, Propellants, Explosives, Pyrotechnics 34 (2009) 385–393.
[6] G. Young, R. Balar, M. Krasel, K. Yu, in: 14th AIAA/AHI Space Planes and Hypersonic Systems and Technologies Conference, Canberra, Australia, 2006.
[7] G. Young, Metallic Nanoparticles as Fuel Additives in Airbreathing Combustion, PhD Dissertation, University of Maryland, Mechanical Engineering, College Park, 2007.
[8] B. Van Devener, S.L. Anderson, Energy & Fuels 20 (2006) 1886–1894.
[9] B. Van Devener, J.P.L. Perez, J. Jankovich, S.L. Anderson, Energy & Fuels 23 (2009) 6111–6120.
[10] B. Van Devener, J.P.L. Perez, S.L. Anderson, Journal of Materials Research 24 (2009) 3462–3464.
[11] B. Rotavera, A. Kumar, S. Seal, E.L. Petersen, Proceedings of the Combustion Institute 32 (2009) 811–819.
[12] S.U.S. Choi, Journal of Heat Transfer – Transactions of the ASME 131 (2009) 033106.1–9.
[13] W.H. Yu, D.M. France, J.L. Routbort, S.U.S. Choi, Heat Transfer Engineering 29 (2008) 432–460.
[14] X.W. Wang, X.F. Xu, S.U.S. Choi, Journal of Thermophysics and Heat Transfer 13 (1999) 474–480.
[15] E.L. Dreizin, Progress in Energy and Combustion Science 35 (2009) 141–167.
[16] K.K Kuo, L.T DeLuca, Combustion of Energetic Materials, Begell House, Inc., 2002.
[17] J.-C. Liu, J.-H. Jean, C.-C. Li, Journal of the American Ceramic Society 89 (2006) 882–887.
[18] C.K Law, Combustion Physics, Cambridge University Press, 2006.
[19] G. Young, K. Sullivan, M.R. Zachariah, K. Yu, Combustion and Flame 156 (2009) 322–333.
[20] P. Antaki, F.A. Williams, Combustion and Flame 67 (1987) 1–8.
[21] S.-C. Wong, A.-C. Lin, H.-Y. Chi, Symposium (International) on Combustion 23 (1991) 1391–1397.
[22] S.-C. Wong, A.-C. Lin, C.-e. Wu, Combustion and Flame 96 (1994) 304–310.
[23] P.R. Choudhury, Progress in Energy and Combustion Science 18 (1992) 409–427.
[24] S.C. Li, F.A. Williams, F. Takahashi, Symposium (International) on Combustion 22 (1989) 1951–1960.
[25] C.L. Yeh, K.K. Kuo, Progress in Energy and Combustion Science 22 (1996) 511–541.
[26] E. Beloni, V.K. Hoffmann, E.L. Dreizin, Journal of Propulsion and Power 24 (2008) 1403–1411.
[27] A. Lee, C.K. Law, Combustion Science and Technology 86 (1992) 253–265.
[28] C.K. Law, Progress in Energy and Combustion Science 8 (1982) 171–201.
[29] Knozinge.H, Angewandte Chemie. International Edition 7 (1968) 791–805.